Biosensors and Bioelectronics 133 (2019) 230–235

Contents lists available at ScienceDirect

Biosensors and Bioelectronics

journal homepage: www.elsevier.com/locate/bios

An electrochemical sensing platform based on ladder-shaped DNA structure and label-free aptamer for ultrasensitive detection of ampicillin

Seyed Mohammad Taghdisi[a,b,1], Noor Mohammad Danesh[c,1], Morteza Alinezhad Nameghi[d], Mohammad Ramezani[d], Mona Alibolandi[d], Khalil Abnous[d,e,*]

[a] Targeted Drug Delivery Research Center, Pharmaceutical Technology Institute, Mashhad University of Medical Sciences, Mashhad, Iran
[b] Department of Pharmaceutical Biotechnology, School of Pharmacy, Mashhad University of Medical Sciences, Mashhad, Iran
[c] Research Institute of Sciences and New Technology, Mashhad, Iran
[d] Pharmaceutical Research Center, Pharmaceutical Technology Institute, Mashhad University of Medical Sciences, Mashhad, Iran
[e] Department of Medicinal Chemistry, School of Pharmacy, Mashhad University of Medical Sciences, Mashhad, Iran

ARTICLE INFO

Keywords:
Aptamer
Ampicillin
Electrochemical sensor
Milk sample
Ladder-shaped DNA structure
Ultrasensitive determination

ABSTRACT

Herein, an electrochemical aptasensor is described for detection of ampicillin (Ampi). The sensing strategy is based on the application of a ladder-shaped DNA structure as a multi-layer physical block on the surface of gold electrode. Attributing to the electrostatic repulsion and physical prevention of the ladder-shaped DNA structure, ultrasensitive detection of Ampi was achieved with a detection limit as low as 1 pM. In the presence of Ampi, the ladder-shaped DNA structure is disassembled and detached from the electrode surface. This leads to the high access of $[Fe(CN)_6]^{3-/4-}$ as a redox indicator to the electrode surface and a strong redox peak. The aptasensor response for Ampi detection was in the linear range from 7 pM to 100 nM with the detection limit of 1 pM. The presented analytical strategy showed its application in detecting Ampi in the spiked milk samples with satisfactory performance. This work can be easily expanded for different targets by alternating the corresponding aptamers.

1. Introduction

Ampicillin (Ampi) is a β-lactam antibiotic which is broadly applied in human and veterinary medicine for treatment and prevention of infectious diseases (Lian et al., 2018; Zhou et al., 2018). Its excessive use can lead to the presence of Ampi in various substances, such as water and milk samples (Yu et al., 2018). So, determination of Ampi residues in food products is essential to protect human health because Ampi can result in adverse effects, including allergic reactions and seizures (Ge et al., 2019).

Common quantitative approaches for Ampi and other antibiotics detection are: high-performance liquid chromatography (HPLC) (Tang et al., 2016), liquid chromatography-mass spectrometry (LC-MS) (Kipper et al., 2017), microbial screening (Chakraborty et al., 2018), Raman spectroscopy (Clarke et al., 2005) and enzyme-linked immunosorbent assays (ELISA) (Ramatla et al., 2017). HPLC and LC-MS suffer from disadvantages like long sample analysis, sophisticated equipment and skilled personnel (Kaur et al., 2017; Zhou et al., 2018b). Microbiological approach is time-consuming and lacks selectivity and high sensitivity (Zhou et al., 2018a). Also, Raman spectroscopy has disadvantages like low sensitivity, slow imaging by point scanning and needs sophisticated data analysis (Eberhardt et al., 2015). Moreover, ELISA has drawbacks such as high possibility of false positive/negative, instability of antibody and high cost (Sakamoto et al., 2018). Consequently, sensing platforms are needed which can provide rapid, simple and sensitive recognition of Ampi residue in foodstuffs.

Recently, aptamers as potent substitutes to antibiotics have been increasingly applied in establishing different sensors. Aptamers are synthetic short single-stranded DNA (ssDNA) or RNA sequences with unique three-dimensional (3D) structures which allow these oligonucleotides to interact with a broad range of targets (Khoshbin et al., 2018; Taghdisi et al., 2018). These recognition probes are isolated by a combinatorial chemistry technique called SELEX (Systematic Evolution of Ligand by EXponential enrichment) (Liu et al., 2019). Relative to antibiotics, aptamers hold distinct benefits, including flexible labeling and regeneration, in vitro synthesis, high stability and low cost (Abnous et al., 2018; Nie et al., 2018; Wang et al., 2018b).

Among different aptamer-based sensors, electrochemical

* Corresponding author at: Targeted Drug Delivery Research Center, Pharmaceutical Technology Institute, Mashhad University of Medical Sciences, Mashhad, Iran.
E-mail address: abnouskh@mums.ac.ir (K. Abnous).
[1] These authors contributed equally to the work.

https://doi.org/10.1016/j.bios.2019.03.044
Received 15 January 2019; Received in revised form 20 March 2019; Accepted 21 March 2019
Available online 22 March 2019
0956-5663/

aptasensors have become widespread for biosensing by virtue of their rapid response, inexpensive instruments, easy miniaturization and high detection sensitivity (Nie et al., 2018; Zhu et al., 2019).

Herein, a novel and ultrasensitive ladder-shaped electrochemical aptasensor was introduced for detection of Ampi. So far, different electrochemical aptasensors have been developed by our group which were based on different shapes, like arch-shape (Danesh et al., 2016), H-shape (Abnous et al., 2016), π-shape (Abnous et al., 2017) and M-shape (Taghdisi et al., 2016). Compared to these approaches, in the absence of target (Ampi), there are multiple layers of ssDNAs on the gold electrode surface of the presented aptasensor which efficiently prohibit the access of the redox couple, $[Fe(CN)_6]^{3-/4-}$, to the surface of electrode via electrostatic repulsion and physical prevention. While in the presence of Ampi, these DNA multiple layers leave the surface of electrode in a relatively short time (60 min) owing to high affinity of aptamer towards its target, leading to high access of redox agent to the electrode surface. Therefore, there is a very big difference between the access of $[Fe(CN)_6]^{3-/4-}$ to the electrode surface in the presence and absence of target, resulting in the ultrasensitive detection of Ampi. Also, Ampi aptamer sequence (Luo et al., 2017; Wang et al., 2016) did not have any modification which could improve its affinity towards Ampi.

2. Materials and methods

2.1. Materials

All DNA sequences were synthesized by Microsynth (Switzerland) (Table S1). Ampicillin (Ampi), potassium hexacyanoferrate(III) ($K_3[Fe(CN)_6]$), amoxicillin (Amox), levofloxacin (Levo), Tris(2-carboxyethyl) phosphine hydrochloride (TCEP), chloramphenicol (Chl), 6-mercapto-hexanol (MCH), kanamycin (Kana), Potassium hexacyanoferrate(II) trihydrate ($K_4[Fe(CN)_6]\cdot 3H_2O$) and tetracycline (Tet) were obtained from Sigma-Aldrich (USA).

2.2. Instrumentation and electrochemical evaluation

μSTAT 400 portable BiPotentiostat/Galvanostat (DropSens, Spain) was utilized for electrochemical experiments using screen-printed gold electrodes (SPGEs, DRP-C220BT, DropSens, Spain) and DropView8400 software.

The electrochemical experiments were measured in the mixture of 0.1 M KCl and 3 mM $[Fe(CN)_6]^{3-/4-}$) as a redox agent. The electrochemical responses were assessed with cyclic voltammetry (CV) in the potential range from − 0.48 to 0.8 V at a scan rate of 50 mV/s and differential pulse voltammetry (DPV) in the potential range from 0.05 to 0.24 V, pulse potential of 10 mV and pulse time of 25 ms.

A JPK NanoWizard II microscope (Germany) and a TESCAN MIRA3 microscope (Czech Republic) were used for atomic force microscopy (AFM) and scanning electron microscopy (SEM), respectively.

2.3. Modification of electrode with aptamer and ssDNAs (ladder-shaped DNA structure) and Ampi analysis

ssDNAs 1 and 6 were firstly dissolved in 10 mM Tris-HCl buffer (containing 5 mM TCEP, 100 mM NaCl, 1 mM EDTA, pH 7.4) to the final concentration of 250 nM for each strand and incubated at room

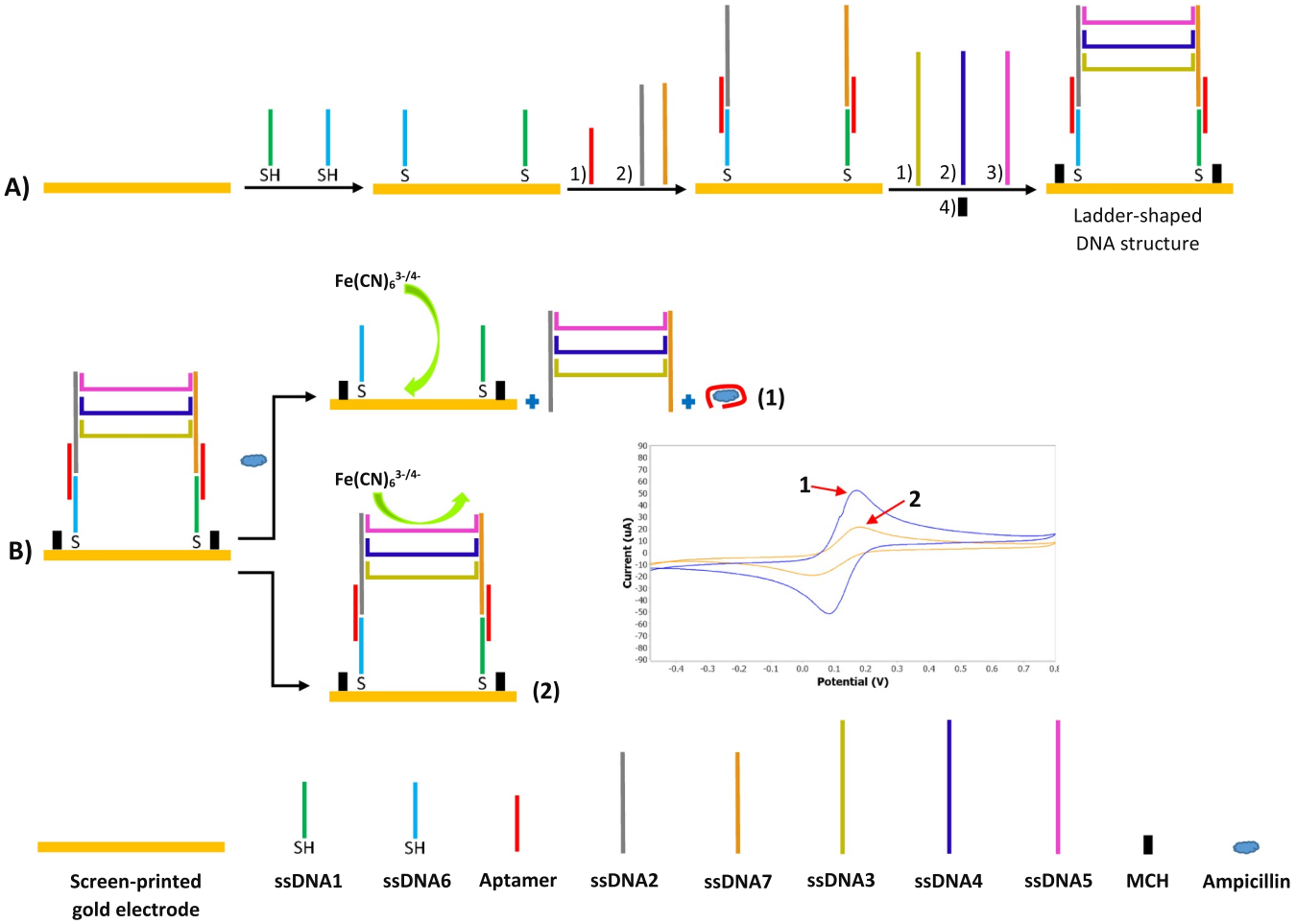

Scheme 1. Schematic diagram of the fabrication procedure of the ladder-shaped DNA structure on the surface of electrode (A) and the function of the electrochemical aptasensor (B).

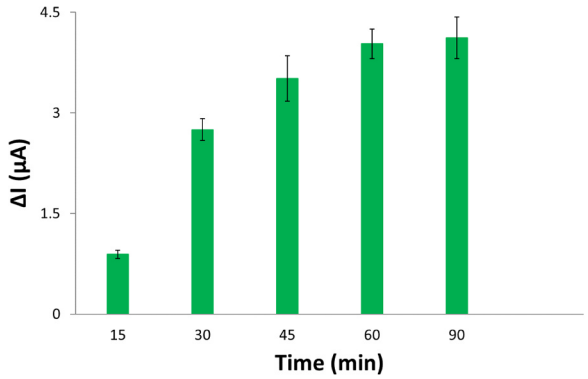

Fig. 1. Effect of the incubation time of the Ampi on the relative electrochemical response ($I-I_0$) of the aptasensor. I_0 and I are the currents before and after addition of Ampi, respectively.

temperature for 1 h to reduce disulfide bonds. The gold electrode was immersed in 10 μL of the above mixture for 10 h at room temperature in a moisture-saturated environment for immobilization of ssDNAs1 and 6 on the gold electrode surface. After that, the electrode surface was rinsed with Tris-HCl (pH 7.4) and 10 μL Ampi aptamer (500 nM) was placed on the surface of electrode for 1.5 h at room temperature, followed by rinsing the surface of electrode. Then, 10 μL solution containing ssDNAs 2 (250 nM) and 7 (250 nM) was dropped onto the electrode surface for 1.5 h at room temperature. Next, 10 μL ssDNAs 3, 4 and 5 (the concentration of each strand was 250 nM) were separately added to the electrode surface and each strand was incubated for 1.5 h. Afterwards, the electrodes were washed with Tris-HCl (pH 7.4) and treated with 10 μL MCH (0.5 mM) for blocking reaction.

The fabricated electrodes were immersed in phosphate buffer saline solution (10 mM PBS) containing various amounts of Ampi (0–200 nM) for 60 min at room temperature. Then, the electrodes were rinsed and DPV analysis was performed.

2.4. Selectivity evaluation of the aptasensor

The specificity of the sensing method was assessed by challenging it with several antibiotics, including Amox, Levo, Chl, Kana and Tet as mentioned above. The concentration of each antibiotic was 100 nM.

2.5. Detection of Ampi in milk samples

Different Ampi concentrations (0–200 nM) were spiked into 10-fold diluted milk samples and the presence of Ampi was determined and analyzed using the ladder-shaped electrochemical aptasensor through DPV.

3. Results and discussion

3.1. Analytical principle

The principle of the presented analytical method was based on a ladder-shaped structure on the surface of electrode, composed of several ssDNAs which could act as a multi-layer physical block for the access of redox couple to the gold electrode surface (Scheme 1). In this sensing platform, the Ampi aptamer is essential for the formation and immobilization of the ladder-shaped DNA structure on the surface of gold electrode.

In the absence of Ampi, the ladder-shaped structure stands unbroken on the surface of electrode and prevents the entry of $[Fe(CN)_6]^{3-/4-}$ to the electrode surface through physical blockage and electrostatic repulsive force between the negatively charged phosphate groups of the immobilized ssDNAs and aptamer and the negatively charged redox probe (Chen et al., 2014; Zhao et al., 2015). So, a weak peak current is observed. Upon adding Ampi, preferential binding of aptamer towards its target leads to release of some parts of the ladder-shaped DNA structure from the electrode surface. Consequently, the redox agent can freely reach the electrode surface. Therefore, the current response is significantly improved.

A)

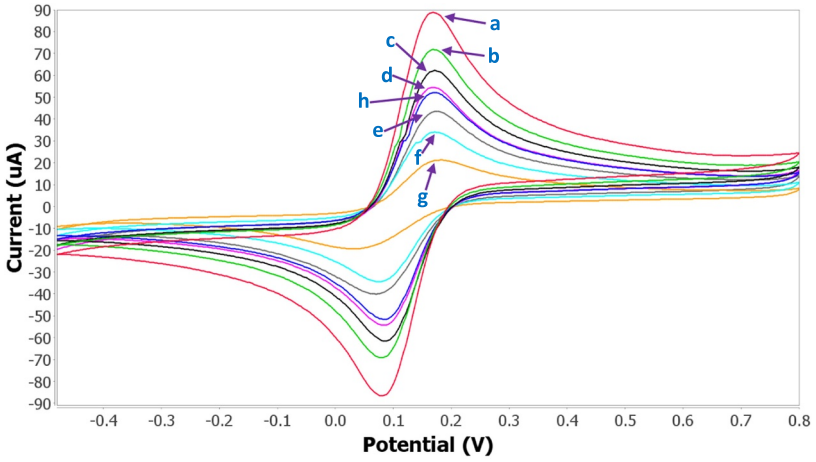

B)

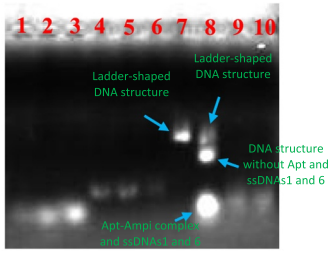

Fig. 2. (A) CV of the electrode fabrication process and aptasensor function. Bare electrode (red curve, a curve), ssDNAs1 and 6 (green curve, b curve), ssDNAs1 and 6 + Aptamer (black curve, c curve), ssDNAs1 and 6 + Aptamer + ssDNAs2 and 7 (pink curve, d curve), ssDNAs1 and 6 + Aptamer + ssDNAs2 and 7 + ssDNA3 (gray curve, e curve), ssDNAs1 and 6 + Aptamer + ssDNAs2 and 7 + ssDNA3 + ssDNA4 (pale blue curve, f curve), ssDNAs1 and 6 + Aptamer + ssDNAs2 and 7 + ssDNA3 + ssDNA4 + ssDNA5 (ladder-shaped structure) (orange curve, g curve), ladder-shaped structure + Ampi (deep blue curve, h curve). (B) Analysis of the formation of the ladder-shaped DNA structure and performance of the aptasensor using agarose gel electrophoresis (2.5%, stained with GelRed). Lane 1: ssDNA1, lane 2: ssDNA6, lane 3: aptamer, lane 4: ssDNA3, lane 5: ssDNA4, lane 6: ssDNA5, lane 7: ladder-shaped DNA structure (ssDNAs1-7 + aptamer), lane 8: ladder-shaped DNA structure + Ampi, lane 9: ssDNA2 and lane 10: ssDNA7.

3.2. Optimization of the incubation time of Ampi

To maximize the electrochemical performance of the aptasensor for Ampi determination, the incubation time of target was examined (Fig. 1). With the increase of incubation time of Ampi, the relative electrochemical signal enhanced. The maximum relative signal was achieved within 60 min and this time was selected for other experiments.

3.3. Verification of the electrode modification and feasibility of the sensing strategy

CV was evaluated under various fabrication procedures to prove that the electrochemical sensing method was fabricated successfully and functioned well. (Fig. 2A). The bare gold electrode presented the maximum redox current (red curve, a curve), indicating free electron transfer of the $[Fe(CN)_6]^{3-/4-}$ at the bare gold electrode. The peak current decreased gradually when ssDNAs 1 and 6 (green curve, b curve), aptamer (black curve, c curve) and ssDNAs 2 and 7 (pink curve, d curve) were successfully immobilized on the electrode surface, respectively. These decreases were caused by the steric hindrance and electrostatic repulsion effects of the negatively charged ssDNAs. The current signal was further reduced following the additions of ssDNAs 3 (gray curve, e curve), 4 (pale blue curve, f curve) and 5 (orange curve, g curve), principally arisen from the formation of the ladder-shaped DNA structure as a multi-layer physical barrier on the surface of electrode and so, poor access of the redox probe to the electrode surface. The CV curve exhibited a strong enhancement when Ampi existed in the sample (deep blue curve, h curve). This was ascribed to the formation of Aptamer-Ampi complex and the release of multiple-layer barrier from the electrode surface due to the stronger binding force between the aptamer and its target (Xi et al., 2018; Zhang et al., 2018; Zhong et al., 2018). Therefore, the transduction of the electron enhanced.

Also the immobilizations of the ssDNAs1 and 6, which is the first step for the formation of the ladder-shaped structure, were investigated using AFM and SEM studies. AFM images revealed that the electrode roughness enhanced from 314.5 nm to 435.7 nm following immobilizations of ssDNAs 1 and 6 (Fig. S1). Also, SEM images showed a change in the morphology of electrode following the additions of ssDNAs1 and 6 (Fig. S2). These results substantiated successfully immobilizations of ssDNAs1 and 6 on the surface of electrode.

The formation and efficiency of the designed aptasensor were also validated by agarose gel electrophoresis analysis (Fig. 2B). Only one major band was detected for ladder-shaped DNA structure (lane 7) and this band displayed lower mobility shift compared to other ssDNAs, suggesting the successful self-assembly of the DNA structure. Upon addition of Ampi, the ladder-shaped DNA structure was disassembled (lane 8), verifying the successful function of the aptasensor in the presence of target.

3.4. Quantitative analysis of Ampi

To evaluate the linear range of the sensing platform and its detection sensitivity towards Ampi, the concentration titration measurements were conducted through DPV. Upon addition of various amounts of Ampi into the detection system, the redox current enhanced with increasing the Ampi concentration (Fig. 3A) which was originated from more disassembly of the ladder-shaped DNA structure with increasing of the Ampi amount. The relative electrochemical response was linear with the logarithm of the concentration of Ampi from 7 pM to 100 nM (Fig. 3B). The detection limit (LOD) was measured to be 1 pM (S/N = 3).

As displayed in Table 1, the analytical performance of the presented aptasensor is superior or comparable with the previous analytical approaches for detection of Ampi. Also, its target detection time is acceptable.

3.5. Selectivity of the aptasensor

The specificity of the aptasensor was analyzed by comparing the current changes induced by Ampi and different antibiotics, including Amox, Levo, Chl, Kana and Tet under the same experimental conditions. Fig. 3C indicates that the remarkable relative electrochemical signal change could only be observed by Ampi. These results obviously showed that the developed aptasensor provided high selectivity for Ampi determination.

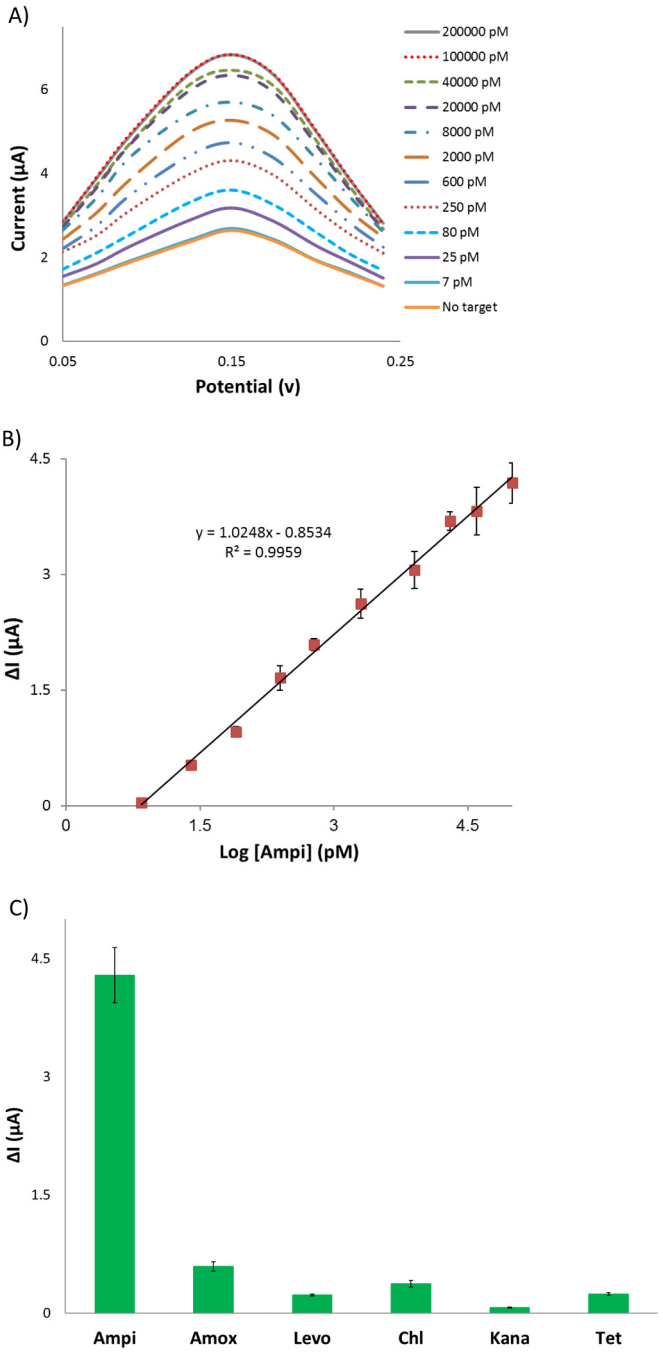

Fig. 3. (A) DPV response of the sensing method after adding different concentrations of Ampi (0–200 nM). (B) Calibration curve of the relative electrochemical response ($I-I_0$) to Ampi. I_0 and I are the currents before and after addition of Ampi, respectively. (C) Relative electrochemical signals of the aptasensor after addition of Ampi, Amox, Levo, Chl, Kana and Tet. I_0 and I are the currents before and after addition of each antibiotic.

Table 1
Comparison of the presented aptasensor with other reported Ampi sensing methods.

Method	LOD	Linear range	Analysis time of Ampi	Reference
A reagentless and reusable electrochemical aptamer-based sensor	1 μM	5–5000 μM	10 min	(Yu and Lai, 2018)
A fluorescent aptasensor using magnetic bead composites coated with gold nanoparticles and a nicking enzyme	0.07 μg/L	0.1–100 μg/L	180 min	(Luo et al., 2017)
A homogeneous electrochemical aptasensor based on dual recycling amplification strategy	4 pM	20 pM – 40 nM	90 min	(Wang et al., 2016)
Label-free detection of ampicillin using silver nanoparticles as a colorimetric sensing probe	10 μg/L	25–1200 μg/L	5 min	(Shrivas et al., 2017)
An Aptamer based voltammetric determination using a single-stranded DNA binding protein and DNA functionalized gold nanoparticles	0.38 pM	1 pM – 5 nM	300 min	(Wang et al., 2018a)
Molecularly imprinted electrochemical sensor based on a gold nanoparticle and multiwalled carbon nanotube-coated Pt electrode	1 nM	10 nM–5 μM	5 min	(Wei et al., 2014)
A detection system using programmable hairpin probes based on a simple double-T type microchip electrophoresis platform and isothermal polymerase-catalyzed target recycling	50 pM	50 pM – 10 nM	62 min	(Zhou et al., 2018b)
Silver Nanoparticles Inkjet-printed Flexible Biosensor	10 mg/L	Not reported	6 min	(Rosati et al., 2019)
Our electrochemical aptasensor	1 pM (0.371 ng/L)	7 pM – 100 nM	60 min	

Table 2
Recovery of Ampi from milk samples (n = 4). Data are mean ± standard deviation (SD).

Milk samples	Added Ampi (nM)	Found (nM)	Recovery (%)	RSD (%, n = 4)
1	0.4	0.37	92.5	5.6
2	0.5	0.47	94	2.5
3	0.9	0.95	105.5	3.8
4	10	10.6	106	3
5	30	29.46	98.2	4.6
6	50	52	104	7.4

3.6. Analysis of milk samples

To assess the applicability of the sensing method in practical analysis, the aptasensor was applied to analyze milk samples containing different concentrations of Ampi. The calibration plot indicated a good relationship in the dynamic range of 100 pM–70 nM for Ampi (Fig. S3). The LOD was determined to be 10 pM (3.713 ng/L), which is much lower than the maximum permitted Ampi content in milk set by European Union (4 μg/kg) (Kaiser et al., 2018; Rosati et al., 2019) and US Food and Drug Administration (FDA, 28.6 nM) (Yu et al., 2018).

Also, to study the accuracy and reproducibility of the aptasensor, the recovery assay was conducted for milk samples spiked with Ampi using the modified gold electrodes which have been prepared in different days. As seen in Table 2, the recoveries of Ampi were between 92.5% and 106% with relative standard deviations (RSDs) less than 7.5%. These results confirmed that the proposed approach was capable of detecting Ampi in real samples with high precision and accuracy.

4. Conclusion

In summary, a novel electrochemical aptasensor was reported for detection of Ampi based on a ladder-shaped DNA structure. The presented sensing strategy not only possessed high specificity towards its target, but also achieved highly sensitive quantitative determination of Ampi with detection limit of 1 pM, which could be ascribed to the presence of a physical bar containing multiple ssDNAs layers on the surface of electrode in the absence of Ampi. Furthermore, the analytical approach was further utilized to detect Ampi in milk samples and the aptasensor showed the recovery rate from 92.5% to 106%, confirming its potential application for Ampi determination in complicated biological samples. However, the preparation of the ladder-shaped DNA structure on the surface of electrode needs multiple steps, increasing the preparation time of the aptasensor. Considering the above characteristics, the developed sensing method can be extended to different targets for which suitable aptamers are available.

CRediT authorship contribution statement

Seyed Mohammad Taghdisi: Formal analysis, Data curation. **Khalil Abnous:** Project administration, Funding acquisition.

Acknowledgment

Financial support of this study was provided by Mashhad University of Medical Sciences.

Conflict of interest

There is no conflict of interest about this article.

Declaration of interests

None.

Authors' contributions

All all authors have read and approved the final manuscript.

Lead author: Name: *Seyed Mohammad Taghdisi*

Disclosure: *His role was in the performance and writing of the manuscript, formal analysis and data curation. He has no conflict of interest about this article.*

Lead author: Name: *Noor Mohammad Danesh*

Disclosure: *His role was in the performance and writing of the manuscript. He has no conflict of interest about this article.*

Corresponding author: Name: Khalil Abnous

Disclosure: *His role was in the development of the idea of the work, project administration, funding acquisition, guidance and reading of the manuscript and its correction. He has no conflict of interest about this article.*

Coauthor: Name: *Mohammad Ramezani*

Disclosure: *His role was in the guidance and reading of the manuscript and its correction. He has no conflict of interest about this article.*

Coauthor: Name: Morteza Alinezhad Nameghi

Disclosure: *His role was in the performance of some parts of the manuscript and reading of the manuscript and its correction. He has no conflict of interest about this article.*

Coauthor: Name: *Mona Alibolandi*

Disclosure: *Her role was in the performance of some parts of the manuscript and reading of the manuscript and its correction. She has no conflict of interest about this article.*

Appendix A. Supporting information

Supplementary data associated with this article can be found in the online version at doi:10.1016/j.bios.2019.03.044.

References

Abnous, K., Danesh, N.M., Alibolandi, M., Ramezani, M., Sarreshtehdar Emrani, A., Zolfaghari, R., Taghdisi, S.M., 2017. A new amplified π-shape electrochemical aptasensor for ultrasensitive detection of aflatoxin B1. Biosens. Bioelectron. 94, 374–379.

Abnous, K., Danesh, N.M., Ramezani, M., Alibolandi, M., Emrani, A.S., Lavaee, P., Taghdisi, S.M., 2018. A colorimetric gold nanoparticle aggregation assay for malathion based on target-induced hairpin structure assembly of complementary strands of aptamer. Microchim. Acta 185 (4).

Abnous, K., Danesh, N.M., Ramezani, M., Taghdisi, S.M., Emrani, A.S., 2016. A novel electrochemical aptasensor based on H-shape structure of aptamer-complimentary strands conjugate for ultrasensitive detection of cocaine. Sens. Actuators B: Chem. 224, 351–355.

Chakraborty, K., Thilakan, B., Kizhakkekalam, V.K., 2018. Antibacterial aryl-crowned polyketide from Bacillus subtilis associated with seaweed Anthophycus longifolius. J. Appl. Microbiol. 124 (1), 108–125.

Chen, D., Yao, D., Xie, C., Liu, D., 2014. Development of an aptasensor for electrochemical detection of tetracycline. Food Control 42, 109–115.

Clarke, S.J., Littleford, R.E., Smith, W.E., Goodacre, R., 2005. Rapid monitoring of antibiotics using Raman and surface enhanced Raman spectroscopy. Analyst 130 (7), 1019–1026.

Danesh, N.M., Ramezani, M., Emrani, A.S., Abnous, K., Taghdisi, S.M., 2016. A novel electrochemical aptasensor based on arch-shape structure of aptamer-complimentary strand conjugate and exonuclease I for sensitive detection of streptomycin. Biosens. Bioelectron. 75, 123–128.

Eberhardt, K., Stiebing, C., Matthaüs, C., Schmitt, M., Popp, J., 2015. Advantages and limitations of Raman spectroscopy for molecular diagnostics: an update. Expert Rev. Mol. Diagn. 15 (6), 773–787.

Ge, L., Xu, Y., Ding, L., You, F., Liu, Q., Wang, K., 2019. Perovskite-type BiFeO3/ultrathin graphite-like carbon nitride nanosheets p-n heterojunction: boosted visible-light-driven photoelectrochemical activity for fabricating ampicillin aptasensor. Biosens. Bioelectron. 124–125, 33–39.

Kaiser, L., Weisser, J., Kohl, M., Deigner, H.P., 2018. Small molecule detection with aptamer based lateral flow assays: applying aptamer-C-reactive protein cross-recognition for ampicillin detection. Sci. Rep. 8 (1).

Kaur, S., Garg, M., Mittal, S., Wangoo, N., Sharma, R.K., 2017. Copper based facile, sensitive and low cost colorimetric assay for ampicillin sensing and quantification in nano delivery system. Sens. Actuators B: Chem. 248, 234–239.

Khoshbin, Z., Verdian, A., Housaindokht, M.R., Izadyar, M., Rouhbakhsh, Z., 2018. Aptasensors as the future of antibiotics test kits-a case study of the aptamer application in the chloramphenicol detection. Biosens. Bioelectron. 122, 263–283.

Kipper, K., Lillenberg, M., Herodes, K., Nei, L., Haiba, E., 2017. Simultaneous determination of fluoroquinolones and sulfonamides originating from sewage sludge compost. Sci. World J. 2017.

Lian, W., Liang, J., Shen, L., Jin, Y., Liu, H., 2018. Enzymatic logic calculation systems based on solid-state electrochemiluminescence and molecularly imprinted polymer film electrodes. Biosens. Bioelectron. 100, 326–332.

Liu, D., Zhang, Z., Yin, Y., Jia, F., Wu, Q., Tian, P., Wang, D., 2019. Development and evaluation of a novel in situ target-capture approach for aptamer selection of human noroviruses. Talanta 193, 199–205.

Luo, Z., Wang, Y., Lu, X., Chen, J., Wei, F., Huang, Z., Zhou, C., Duan, Y., 2017. Fluorescent aptasensor for antibiotic detection using magnetic bead composites coated with gold nanoparticles and a nicking enzyme. Anal. Chim. Acta 984, 177–184.

Nie, J., Yuan, L., Jin, K., Han, X., Tian, Y., Zhou, N., 2018. Electrochemical detection of tobramycin based on enzymes-assisted dual signal amplification by using a novel truncated aptamer with high affinity. Biosens. Bioelectron. 122, 254–262.

Ramatla, T., Ngoma, L., Adetunji, M., Mwanza, M., 2017. Evaluation of antibiotic residues in raw meat using different analytical methods. Antibiotics 6 (4).

Rosati, G., Ravarotto, M., Scaramuzza, M., De Toni, A., Paccagnella, A., 2019. Silver nanoparticles inkjet-printed flexible biosensor for rapid label-free antibiotic detection in milk. Sens. Actuators B: Chem. 280, 280–289.

Sakamoto, S., Putalun, W., Vimolmangkang, S., Phoolcharoen, W., Shoyama, Y., Tanaka, H., Morimoto, S., 2018. Enzyme-linked immunosorbent assay for the quantitative/qualitative analysis of plant secondary metabolites. J. Nat. Med. 72 (1), 32–42.

Shrivas, K., Sahu, J., Maji, P., Sinha, D., 2017. Label-free selective detection of ampicillin drug in human urine samples using silver nanoparticles as a colorimetric sensing probe. New J. Chem. 41 (14), 6685–6692.

Taghdisi, S.M., Danesh, N.M., Ramezani, M., Abnous, K., 2016. A novel M-shape electrochemical aptasensor for ultrasensitive detection of tetracyclines. Biosens. Bioelectron. 85, 509–514.

Taghdisi, S.M., Danesh, N.M., Ramezani, M., Sarreshtehdar Emrani, A., Abnous, K., 2018. A simple and rapid fluorescent aptasensor for ultrasensitive detection of arsenic based on target-induced conformational change of complementary strand of aptamer and silica nanoparticles. Sens. Actuators B: Chem. 256, 472–478.

Tang, Y., Li, M., Gao, X., Liu, X., Ma, Y., Li, Y., Xu, Y., Li, J., 2016. Preconcentration of the antibiotic enrofloxacin using a hollow molecularly imprinted polymer, and its quantitation by HPLC. Microchim. Acta 183 (2), 589–596.

Wang, J., Ma, K., Yin, H., Zhou, Y., Ai, S., 2018a. Aptamer based voltammetric determination of ampicillin using a single-stranded DNA binding protein and DNA functionalized gold nanoparticles. Microchim. Acta 185 (1).

Wang, X., Dong, S., Gai, P., Duan, R., Li, F., 2016. Highly sensitive homogeneous electrochemical aptasensor for antibiotic residues detection based on dual recycling amplification strategy. Biosens. Bioelectron. 82, 49–54.

Wang, X., Zhu, Y., Olsen, T.R., Sun, N., Zhang, W., Pei, R., Lin, Q., 2018b. A graphene aptasensor for biomarker detection in human serum. Electrochim. Acta 290, 356–363.

Wei, S., Liu, Y., Hua, T., Liu, L., Wang, H., 2014. Molecularly imprinted electrochemical sensor for the determination of ampicillin based on a gold nanoparticle and multi-walled carbon nanotube-coated pt electrode. J. Appl. Polym. Sci. 131 (16).

Xi, D., Li, Z., Liu, L., Ai, S., Zhang, S., 2018. Ultrasensitive detection of cancer cells combining enzymatic signal amplification with an aerolysin nanopore. Anal. Chem. 90 (1), 1029–1034.

Yu, Z.-G., Lai, R.Y., 2018. A reagentless and reusable electrochemical aptamer-based sensor for rapid detection of ampicillin in complex samples. Talanta 176, 619–624.

Yu, Z.G., Sutlief, A.L., Lai, R.Y., 2018. Towards the development of a sensitive and selective electrochemical aptamer-based ampicillin sensor. Sens. Actuators B: Chem. 258, 722–729.

Zhang, Y., Wu, Q., Sun, M., Zhang, J., Mo, S., Wang, J., Wei, X., Bai, J., 2018. Magnetic-assisted aptamer-based fluorescent assay for allergen detection in food matrix. Sens. Actuators B: Chem. 263, 43–49.

Zhong, Z., Gao, X., Gao, R., Jia, L., 2018. Selective capture and sensitive fluorometric determination of Pseudomonas aeruginosa by using aptamer modified magnetic nanoparticles. Microchim. Acta 185 (8).

Zhao, F., Xie, Q., Xu, M., Wang, S., Zhou, J., Liu, F., 2015. RNA aptamer based electrochemical biosensor for sensitive and selective detection of cAMP. Biosens. Bioelectron. 66, 238–243.

Zhou, J., Nie, W., Chen, Y., Yang, C., Gong, L., Zhang, C., Chen, Q., He, L., Feng, X., 2018a. Quadruplex gold immunochromatogaraphic assay for four families of antibiotic residues in milk. Food Chem. 256, 304–310.

Zhou, L., Gan, N., Wu, Y., Hu, F., Lin, J., Cao, Y., Wu, D., 2018b. Multiplex detection of quality indicator molecule targets in urine using programmable hairpin probes based on a simple double-T type microchip electrophoresis platform and isothermal polymerase-catalyzed target recycling. Analyst 143 (11), 2696–2704.

Zhu, C., Zhu, W., Xu, L., Zhou, X., 2019. A label-free electrochemical aptasensor based on magnetic biocomposites with Pb2+-dependent DNAzyme for the detection of thrombin. Anal. Chim. Acta 1047, 21–27.